Semiconductors, 2023, Vol. 57, No. 8

Development of a method for etching the InAs/InAsSbP photodiode heterostructures

© A.A. Pivovarova, N.D. Il'inskaya, E.V. Kunitsyna, Yu.P. Yakovlev

Ioffe Institute,
194021 St. Petersburg, Russia

E-mail: Pivovarova.antonina@iropto.ioffe.ru

Received July 4, 2023
Revised October 25, 2023
Accepted November 4, 2023

A method for etching the InAs/InAsSbP photodiode heterostructures using a new precision etchant HBr : $KMnO_4$ with a low constant etching rate was proposed. The change in the ratio of the etchant components makes it possible to set the etching rate in the range of $0.1-1.6\,\mu$m/min without deterioration of the quality of the side semiconductor surface. The use of the new etchant resulted in reducing the reverse dark currents of the InAs/InAsSbP photodiodes as well as the spread of dark current value from the device to the device. Samples with a sensitive area diameter of $300\,\mu$m demonstrate the minimum current density $j = 5.7 \cdot 10^{-2}$ A/cm^2 and the typical current density $j = 15.5 \cdot 10^{-2}$ A/cm^2. The maximum value of R_0 at room temperature is 1654 Ohm, while the R_0A product reaches 1.17 Ohm $\cdot$ cm^2.

Keywords: indium arsenide, photodiode, new etchant, reverse dark currents, differential resistance.

DOI: 10.61011/SC.2023.08.57626.5391

1. Introduction

Photodiodes based on InAs and its solid solutions, which have spectral sensitivity in the mid-IR range, are successfully used as optoelectronic components in gas analysis systems, in particular in modern systems of non-contact radiation thermometry [1], as well as in CH_4, CO and other gases analyzers [2]. The portability and low power consumption of such devices allow to use them in monolithic evanescent wave sensors for various liquids [3]. The emergence of flexible thin-film photodiodes based on InAs opens up prospects for the development of modern portable medical monitoring systems and new generation biomedical thermal imagers [4].

When creating photodiodes based on narrow-gap InAs material ($E_g = 0.36$ eV at $T = 300$ K), an important problem is the development of post-growth technology that ensures minimal variation in parameters from device to device. One of the key intervals of post-growth technology is — chemical etching of a semiconductor. It is important that this process is controlled and, if required, carried out with precision accuracy, and also does not degrade the parameters of the instruments.

It is known that for InAs-based materials there is an effect of revealing lattice planes, which manifests itself to one degree or another for most known etchants. The {111}A plane, consisting of In atoms, is the least active, since all the valence electrons of the atoms forming it are in a bound state. In turn, the {111}B plane, consisting of As atoms, each of which has two unpaired electrons, has a higher reactivity [5]. Thus, at local etching, the relief is determined by the planes with the lowest etching rate, which greatly affects the shape of the resulting mesa-structure. This effect is at etching in $H_3PO_4 : H_2O_2 : H_2O$ (1 : 1 : 1) [6], as well as $H_2SO_4 : H_2O_2 : H_2O$ (3 : 1 : 1) [7].

For InAs-based semiconductors, the Br_2-HBr [8] system is widely used, which allows the formation of round mesa-structures with a reflecting side wall. One way to obtain such a system is to add an oxidizing agent to hydrobromic acid HBr. Meanwhile, a chemical reaction occurs: the oxidation of HBr to the formation of free bromine Br_2. As a result, the etchant contains hydrobromic acid, some oxidizing agent, water and free bromine. The amount of Br_2 depends on the concentration and oxidation potential of the introduced oxidant, which can be an aqueous solution of potassium bichromate $K_2Cr_2O_7$ [9], nitric acid HNO_3 [10], bichromate ammonium $(NH_4)_2Cr_2O_7$ [11] etc. The most common oxidizing agent is hydrogen peroxide H_2O_2. However, when such a strong oxidizing agent is added, the etching rate increases significantly [12], and also depends exponentially on time. The introduction of an organic solvent — ethyl alcohol into the etchant HBr : H_2O_2 reduces the etching rate of InAs-based materials by almost twice, however, its exponential dependence on time remains, which does not allow precision etching of the semiconductor [13].

To carry out such technological operations as thinning epitaxial layers, processing a heterostructure before sputtering of contacts, forming a surface relief with high precision, etc. an etchant with a low constant etch rate is required.

It is known that the method of treating the semiconductor surface affects the value of the dark current of photodiodes. In case of low thermal noise of the load resistance and low shot noise, the dark current determines the main component of the noise current and, accordingly, the threshold sensitivity of the photodiode. To compare devices with different areas and bandwidths, a value such as specific threshold sensitivity Φ^* (specific equivalent noise power NEP*) is used: $\Phi^* = \Phi/(A\Delta f) = S_I^{-1} i_n^{1/2}/(A\Delta f)^{1/2}$, where Φ —

threshold sensitivity, S_I — current monochromatic sensitivity, i_n — noise current, A — area of the photosensitive region, Δf — frequency band. Thus, to achieve a minimum noise level, it is necessary for the photodiode to have a low dark current.

In turn, the dark current consists of both volume and surface components. As the area of the photosensitive region decreases, the contribution of the surface component increases and for small areas $A \leq 3.0 \cdot 10^{-4}\,\text{cm}^2$ becomes predominant. The magnitude of the surface component largely depends on the state of the semiconductor surface. It is important to note that when creating photodiodes, not only the magnitude of the dark currents itself matters, but also its spread across the plate from device to device. In serial production, this variation will affect reproducibility, yield percentage and ultimately determine profitability.

In the case of predominance of thermal noise of the photodiode, the specific threshold sensitivity Φ^* is inversely proportional to the square root of the product of the differential (dynamic) resistance of the photodiode and the area of the photosensitive region $(R_0\text{A})^{1/2}$. To achieve the threshold sensitivity of photodetector devices operating in the mid-IR range, the differential resistance of a photodiode based on InAs and its solid solutions should be $\geq 50\,\text{Ohm}$ [14]. Currently, photodiodes have been created with an InAs active region and a maximum sensitivity wavelength $3.3-3.4\,\mu\text{m}$, the R_0 of which at room temperature reaches 1600 Ohm for $\text{A} = 3.46 \cdot 10^{-4}\,\text{cm}^2$ [15]. To obtain the maximum possible values of the parameter R_0A, increasing the area A is not always justified, since it leads to a decrease in the performance of the device. In this regard, the efforts of developers are primarily aimed at increasing the values of R_0, which is inversely proportional to the value of the dark current at zero bias and in practice is defined as $R_0 = (dI/dU)^{-1}$ at $U = \pm 10\,\text{mV}$.

We have proposed a precision etchant based on the $HBr:KMnO_4:H_2O$ system, which uses an aqueous solution of potassium permanganate, which is a weaker oxidizing agent [16]. A detailed study of the developed etchant was carried out in this work. Its influence on the value of dark currents of InAs/InAsSbP photodiodes and the spread of this value from device to device, as well as on the differential resistance, has been studied.

2. Specimens and methods of study

The work was carried out in two intervals. At the first interval, a study was carried out of the dependence of the etching rate n-InAs(100) on the ratio of solution components and on temperature in the proposed system $HBr:KMnO_4:H_2O$.

The etchant was prepared by mixing various volume fractions of an aqueous solution of $KMnO_4$ and concentrated HBr. The experimental technique consisted of etching the topological pattern of the semiconductor through a photoresist mask, followed by measuring the depth of the etched relief using a DektakXT profilometer. The surface quality was assessed using optical and scanning-electron microscopes. To obtain the temperature dependences of the etch rate of n-InAs(100), each component of the etchant was heated to the required temperature, after which the components were mixed, and a sample with a photoresist mask was lowered into the etchant. To lower the temperature of the etchant components below room temperature, ice and a mixture of dioxane and ice were used (melting point of dioxane 12°C).

At the second interval of the work, photodiodes based on InAs/InAsSbP heterostructures were manufactured using a new etchant $HBr:KMnO_4$ and their characteristics were studied.

Photodiode heterostructures n-InAs/p-$InAs_{0.55}Sb_{0.15}P_{0.3}$ were grown by MOVPE method on an n-InAs (100) substrate. Deposition was carried out in a horizontal reactor with resistive heating at atmospheric pressure. When growing solid solutions, organometallic compounds (trimethylindium TMIn, trimethylstibine TMSb) and hydride gases (arsine AsH_3, phosphine PH_3) were used. The ratio between the components of the V and III groups was set by the arsine flow in the reactor; the InAs active region was not doped. Diethylzinc (DEZn) was used as a source of acceptor dopant for InAsSbP. The thickness of the resulting layers was $3\,\mu\text{m}$ for n-InAs and $1.9\,\mu\text{m}$ for p-$InAs_{0.55}Sb_{0.15}P_{0.3}$. Concentration in InAs — $n \sim (3 \cdot 5) \cdot 10^{17}\,\text{cm}^{-3}$; in InAsSbP — $p \sim (1 \cdot 2) \cdot 10^{18}\,\text{cm}^{-3}$.

The photodiodes were fabricated using standard photolithography techniques. Photosensitive area diameter was $300\,\mu\text{m}$. The ohmic contact to the wide-gap InAsSbP layer was formed by high-vacuum thermal layer-by-layer deposition of the Cr–Au–Ni–Au system, followed by thickening by local electrochemical deposition of gold to $2\,\mu\text{m}$. On the side of the substrate, after thinning the latter, a continuous contact was sputtered using the method of high-vacuum thermal sputtering of the Cr–Au–Ni–Au system, followed by sputtering of the Cr–Au system to a total thickness of $\sim 0.6\,\mu\text{m}$. Mesa-structures were etched to a depth of $\sim 7\,\mu\text{m}$. For the convenience of further dividing the plate into chips, liquid etching of the separating grid was also carried out.

Measurements of the photosensitivity spectra of the studied photodiode samples were carried out using a synchronous detection scheme using an SPM2 prism monochromator (Carl Zeiss), a mechanical modulator and a Stanford Research SR830 synchronous detector. The volt-ampere characteristics (VAC) of photodiodes were studied using an automated VAC meter. The graphs were displayed in real time on a computer monitor. Differential resistance R_0, was determined by the slope of the linear section of the current-voltage characteristic without illumination of the photodiode in the range $\pm 10\,\text{mV}$. In practice, this method is also used to determine the typical shunt resistance R_{sh} of photodiodes [17].

To study the effect of the proposed etchant $HBr:KMnO_4$ on the value of reverse dark currents of photodiodes,

devices were manufactured on the same *n*-InAs/*p*-InAsSbP heterostructure. At the etching stage, the plate was divided into two parts, one of which was processed in a standard etchant $HBr:H_2O_2$, and the other — in the developed $HBr:KMnO_4$. A comparative study was carried out on the VAC of photodiodes manufactured using standard and developed etchants.

3. Experimental results and discussion

The obtained dependences of the etching rate of *n*-InAs(100) substrates on the ratio of components (in volume fractions) of the etching solution in the $HBr:KMnO_4:H_2O$ system are presented in Figure 1.

As can be seen from Figure 1, with an increase in the volume fraction of an aqueous solution of potassium permanganate for each of the given concentrations, the etching rate increases, and until the maximum value is reached (the extremum point on the graph), there is a reflecting and smooth etching surface. With a further increase in the volume fraction of the aqueous solution of $KMnO_4$, the etching rate decreases and the quality of the resulting surface deteriorates, and after reaching a certain critical ratio, an insoluble precipitate of manganese reduction products occurs. A decrease in the concentration of the aqueous solution of the oxidizer leads to a decrease in the etching rate. When using 0.7% aqueous solution of potassium permanganate, there was a reflecting surface throughout the entire range studied. It has been shown that, depending on the concentration of the aqueous solution of $KMnO_4$ (from 0.7 to 3%) and its volume fraction in the solution, it is possible to obtain different etching rates — from ~ 0.1 to $\sim 1.6\,\mu$m/min.

The etching of the *p*-InAsSbP quaternary solid solution based on InAs had a similar character, which subsequently also made it possible to obtain a reflecting side surface of the InAs/InAsSbP mesa-structure.

A comparison was made of the dependences of the etching rate on time $V(t)$ for various etchants. Figure 2 shows the dependences for the widely used etchant $HBr:H_2O_2$, (curve *4*), the etchant $HBr:H_2O_2$ with the addition of ethylene glycol (curve *3*) and the etchant $HBr:KMnO_4$ developed by us using 1.5% aqueous solution of $KMnO_4$ (curves *1* and *2*). It is shown that the developed etchant allows one to reduce the etching rate by an order of magnitude, while its significant advantage is the constant etching rate observed at a number of ratios of solution components.

Analysis of the chemical reactions occurring during the preparation of etchants showed that when mixing the components $HBr:H_2O_2$, an interaction reaction occurs, accompanied by strong heating of the solution and the active release of free bromine. The chemical reaction proceeds as follows:

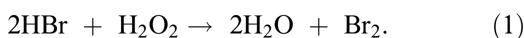

$$2HBr + H_2O_2 \rightarrow 2H_2O + Br_2. \quad (1)$$

As can be seen from reaction (1), when the components of the etchant are combined, part of the HBr is oxidized with

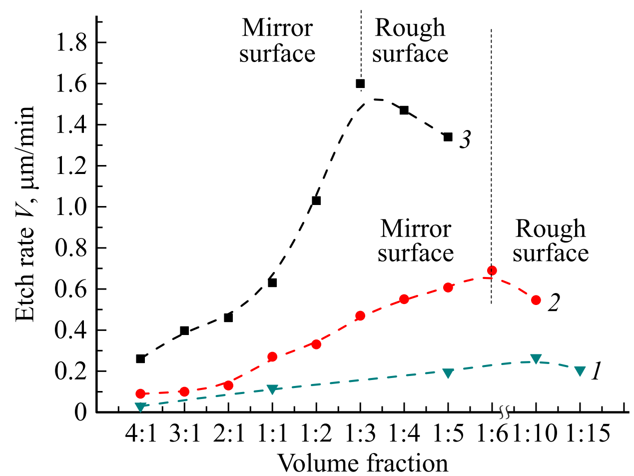

Figure 1. Dependences of the etching rate V for *n*-InAs(100) in the etchant $HBr:KMnO_4$ on the volume fraction of an aqueous solution of potassium permanganate at its various concentrations, %: *1* — 0.7, *2* — 1.5, *3* — 3.

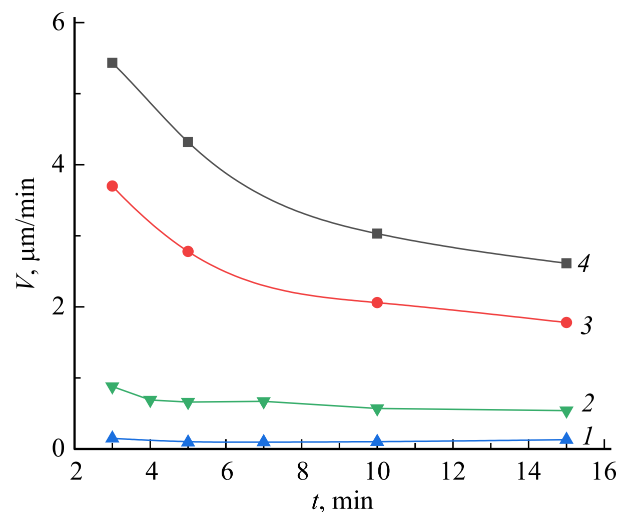

Figure 2. Dependence of etch rate V for *n*-InAs(100) on time t for various etchants: *1* — $HBr:KMnO_4$ (1.5%) 4:1, *2* — $HBr:KMnO_4$ (1.5%) 1:6, *3* — $HBr:H_2O_2$ 8:1, *4* — $HBr:H_2O_2:C_2H_5OH$ 24:3:10.

hydrogen peroxide to water and free bromine molecules. When using an aqueous solution of potassium permanganate as an oxidizing agent, the chemical reaction has the following form:

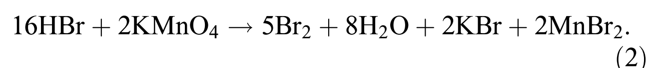

$$16HBr + 2KMnO_4 \rightarrow 5Br_2 + 8H_2O + 2KBr + 2MnBr_2. \quad (2)$$

After mixing the components, their interaction does not lead to significant heating of the solution, and in reaction (2), in addition to water and free bromine, potassium bromide and divalent manganese bromide are additionally formed.

We believe that the linear dependence of the etching rate on time in the developed etchant with a predominant

amount of HBr is due to the establishment of chemical equilibrium and maintaining a constant concentration of the Br_2 oxidizer in the solution.

The activation energy of the etching process n-InAs(100) was determined, the value of which can be used to judge the mechanism of this chemical process. For this purpose, temperature dependences of the etching rate were obtained in the range from 3 to 50°C for two compositions with maximum and minimum etching rates.

The activation energy of the chemical process E_a, related to one mole of reacting particles, was determined from the obtained temperature dependences graphically using the Arrhenius formula [18]:

$$\ln k = \ln k_0 - \frac{E_a}{RT}, \quad (3)$$

where k — rate constant of a chemical reaction, k_0 — frequency factor characterizing the frequency of active collisions of reacting particles per unit volume, R — universal gas constant ($8.314 \cdot 10^{-3}$ kJ/mol · K), T — temperature (K).

For the etchant $HBr:KMnO_4$ 1 : 3 using a 3% aqueous solution of the oxidizer E_a was 12.2 kJ/mol, and for composition 4 : 1 — 7.4 kJ/mol. It is known that for diffusion limitation, in which the etchant is polishing, the characteristic activation energy is $\sim$ 8–20 kJ/mol, and for kinetic limitation, when the etching rate is different for different planes, the value E_a is more than 35–40 kJ/mol [19]. As can be seen, the studied compositions are characterized by a diffusion etching mechanism, in which the InAs surface becomes reflecting.

The etchant used in the manufacture of photodiodes with a given size and shape of the photosensitive area can significantly influence the magnitude of the reverse dark current, namely its surface component, which is caused to varying degrees by various mechanisms: generation and recombination through surface states or in the near-surface depletion region, tunneling through surface states, ohmic shunting of the$p-n$-transition to the surface, etc.

By the results of the studies, a 1.5% aqueous solution of $KMnO_4$ was chosen to create photodiodes based on InAs/InAsSbP heterostructures, which allows to obtain a reflecting semiconductor surface for compositions from 4 : 1 to 1 : 6. Meanwhile, the etching rate was 0.1–0.7 μm/min, depending on the composition of the etchant.

A study of the spectral characteristics of the manufactured InAs/InAsSbP photodiodes showed that all samples have a spectral sensitivity in the range 1.0–3.8 μm.

A study of the volt-ampere characteristics (VAC) of the resulting devices was carried out and the influence of the proposed etchant on the value of reverse dark currents was shown. In Figure 3 typical reverse branches of the current-voltage characteristics of InAs/InAsSbP photodiodes fabricated using the standard etchant $HBr:H_2O_2$ and the developed etchant $HBr:KMnO_4$ are shown.

The table shows the values of the parameters we obtained when analyzing the current-voltage characteristics of InAs/InAsSbP photodiodes for each of the etchants $HBr:H_2O_2$ and $HBr:KMnO_4$.

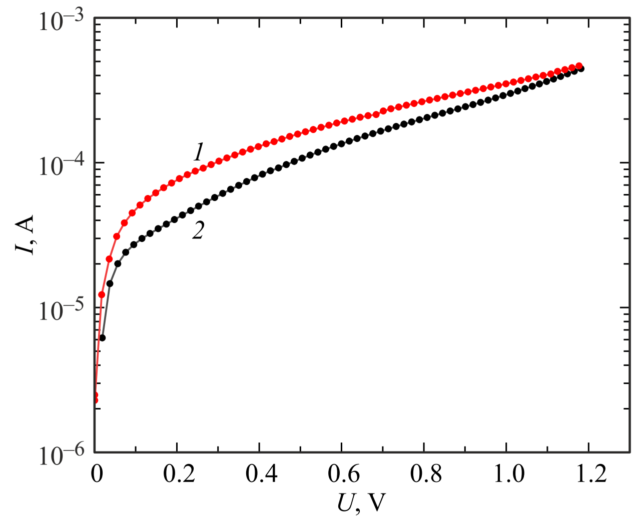

Figure 3. Reverse branches of the current-voltage characteristics of InAs/InAsSbP photodiodes fabricated using etchants: *1* — $HBr:H_2O_2$, *2* — $HBr:KMnO_4$.

As can be seen from the table, the minimum value of the reverse dark current at the reverse bias voltage $U_{rev} = 0.5$ V for the studied samples of InAs/InAsSbP photodiodes is $I_{min} = 80\,\mu$A in the case of the etchant $HBr:H_2O_2$ and $I_{min} = 40\,\mu$A for $HBr:KMnO_4$. Typical values for $U_{rev} = 0.5$ V — $I_{typ} = 157\,\mu$A and $I_{typ} = 107\,\mu$A for the standard and proposed etchants, respectively.

Currently, modern InAs photodiodes with a diameter of 1 mm exhibit a typical reverse dark current $\sim 800\,\mu$A at $U_{rev} = 0.5$ B and $T = 25$°C [20], which corresponds to the current density $j = 10.2 \cdot 10^{-2}$ A/cm^2. The photodiodes presented in this work with a diameter of 300 μm, fabricated using $HBr:KMnO_4$, have a minimum dark current density $j = 5.7 \cdot 10^{-2}$ A/cm^2 and a typical — $j = 15.5 \cdot 10^{-2}$ A/cm^2.

The maximum value of R_0 for such samples is 1654 Ohm with a sensitive area diameter of 300 μm, then the factorR_0A — 1.17 Ohm · cm^2 at room temperature. Typical values of R_0 and (R_0A) increase by 23% compared to R_0 and (R_0A) photodiodes obtained using the standard etchant $HBr:H_2O_2$.

Parameters of InAs/InAsSbP photodiodes

Parameter	Etcher	
	$HBr:H_2O_2$	$HBr:KMnO_4$
I_{min}, μA($U_{rev} = 0.5$ B)	80	40
I_{max}, μA($U_{rev} = 0.5$ B)	920	570
I_{typ}, μA($U_{rev} = 0.5$ B)	157	107
$R_{0\,min}$, Ohm	457	617
$R_{0\,max}$, Ohm	1422	1654
R_{0typ}, Ohm	993	1287

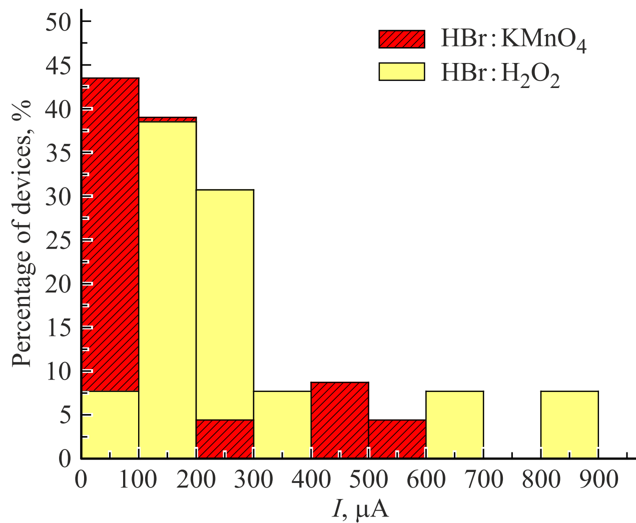

Figure 4. Quantitative distribution of (%) InAs/InAsSbP photodiodes by the magnitude of reverse dark currents at $U_{\text{rev}} = 0.5\,\text{V}$ for various etchants: HBr : $KMnO_4$ — hatching, HBr : H_2O_2 — without hatching.

The results of studying the spread of the reverse dark current from photodiode to photodiode are shown in the histogram (Figure 4). The distribution of samples according to the magnitude of reverse dark currents is demonstrated at a reverse voltage $U_{\text{rev}} = 0.5\,\text{V}$.

As can be seen from Figure 4, when using the developed etchant HBr : $KMnO_4$, 43.5% of photodiodes have a reverse current value $I_{\text{rev}} \leq 100\,\mu\text{A}$, whereas in the case of the standard etchant HBr : H_2O_2 $I_{\text{rev}} \leq 100\,\text{uA}$ — 7.7% of devices. Meanwhile, $I_{\text{rev}} \geq 200\,\mu\text{A}$ is demonstrated by 17.5% of devices when using the developed etchant and 53.8% — the standard one. It should be noted that currents of magnitude $> 600\,\mu\text{A}$ are observed only for photodiodes (15%), created using the etchant HBr : $H_{22}O_2$.

Thus, photodiodes made using HBr : $KMnO_4$ have a smaller scatter of dark current values from device to device and, therefore, greater reproducibility of the results obtained.

4. Conclusion

A new precision etchant HBr : $KMnO_4$ for photodiode InAs/InAsSbP heterostructures has been proposed and studied. The influence of the ratio of its components and the concentration of an aqueous solution of potassium permanganate on the etching rate of InAs-based materials and the quality of the resulting surface was studied. It has been shown that, depending on the concentration of the aqueous solution of $KMnO_4$ and its volume fraction in the solution, it is possible to obtain etching rates from 0.1 to $1.6\,\mu\text{m/min}$. The low and time-constant etching rate in the proposed etchant makes it possible to solve technological problems requiring precision controlled etching of semiconductor materials.

When comparing the current-voltage characteristics of InAs/InAsSbP photodiodes, it was shown that the developed etchant HBr : $KMnO_4$ allows to reduce dark currents and reduce the spread of their values from device to device. Thus, when using the developed etchant, 17.5% of devices demonstrate $I_{\text{rev}} \geq 200\,\mu\text{A}$, and 53.8% of the standard etchant. The created photodiodes have a minimum current density of $j = 5.7 \cdot 10^{-2}\,\text{A/cm}^2$ and a typical — $j = 15.5 \cdot 10^{-2}\,\text{A/cm}^2$.

It has been shown that the use of HBr : $KMnO_4$ allows to increase the values of R_0 and, correspondingly, R_0A by 23%. The R_0A value for the best samples is $1.17\,\text{Ohm} \cdot \text{cm}^2$.

Acknowledgments

The authors would like to thank A.P. Lozhkin for measuring the volt-ampere characteristics of photodiodes.

Conflict of interest

The authors declare that they have no conflict of interest.

References

[1] G.Yu. Sotnikova, S.A. Alexandrov, G.A. Gavrilov. Uspekhi prikl. fiziki, **10** (4), 389 (2022). (in Russian). DOI: 10.51368/2307-4469-2022-10-4-389-403

[2] https://vigophotonics.com/product/pva-3-d1-2-smd-pal2o3-115/#specification

[3] S.A. Karandashev, T.S. Lukhmyrina, B.A. Matveev, M.A. Remennyi, A.A. Usikova, Phys. Status Solidi A: Appl. Mater., **219** (2), ArtNo: 2100456 (2022). DOI: 10.1002/pssa.202100456.

[4] S. Woo, G. Ryu, S.S. Kang, T.S. Kim, N. Hong, J.-H. Han, R.J. Chu, I.-H. Lee, D. Jung, W.J. Choi. ACS Appl. Mater. Interfaces, 2021, **13** (46), 55648 (2021). DOI: 10.1021/acsami.1c14687.

[5] *Fiziko-khimicheskiye metody obrabotki poverkhnosti poluprovodnikov,* pod red. B.D. Luft (M., Radio i svyaz', 1982) p. 37. (in Russian).

[6] A.R.J. Marshall, C.H. Tan, J.P.R. David, J.S. Ng, M. Hopkinson. In: *Fabrication of InAs photodiodes with reduced surface leakage current,* ed. by J.G. Grote, F. Kajzar, M. Lindgren (Proc. SPIE, **6740**, 67400H, 2007). DOI: 10.1117/12.740700.

[7] D. Pasquariello, E.S. Björlin, D. Lasaosa, Y.-J. Chiu, J. Piprek, J.E. Bowers. J. Lighwave Techn., **24** (3), 1470 (2006).

[8] B.A. Matveyev, M.A. Remennyy, A.A. Usikova, N.D. Il'inskaya. *Sposob izgotovleniya diodov srednevolnovogo IK diapazona spektra.* Pat. № 2599905, Rossiyskaya Federatsiya, prioritet izobreteniya 11 maya 2012 g. (in Russian).

[9] A.V. Malevskaya, N.D. Il'inskaya, V.M. Andreev, Pis'ma ZhTF, **45** (24), 14 (2019). (in Russian). DOI: 10.21883/PJTF.2019.24.48795.17953 [A.V. Malevskaya, N.D. Il'inskaya, V.M. Andreev. Tech. Phys. Lett., **45**, 1230 (2019). DOI: 10.1134/S1063785019120241]

[10] A.S. Kurochkin, A.V. Babichev, D.V. Denisov, L.Ya. Karachinsky, I.I. Novikov, A.N. Sofronov, D.A. Firsov, L.E. Vorobjev, A. Bousseksou, A.Yu. Egorov. J. Phys.: Conf. Ser., **993**, 012031 (2018). DOI: 10.1088/1742-6596/993/1/012031

[11] I. Levchenko, V. Tomashyk, G. Malanych, I. Stratiychuk, A. Korchovyi. Appl. Nanoscience, **12**, 1139 (2022). DOI: 10.1007/s13204-021-01784-w

[12] J. Na, S. Lee, S. Lim. Surf. Sci., **658**, 22 (2017). DOI: 10.1016/j.susc.2017.01.002

[13] A.A. Pivovarova, O.YU. Serebrennikova, N.D. Il'inskaya. *Nedelya nauki SPbPU: Mater. nauchnoy konferentsii s mezhdunarodnym uchastiyem* (SPb., Rossiya, 2014) p. 246. (in Russian).

[14] G.A. Gavrilov, B.A. Matveev, G.Y. Sotnikova. Phys. Lett., **37** (9), 866 (2011). DOI: 10.1134/S1063785011090197

[15] N. Dyakonova, S.A. Karandashev, M.E. Levinshtein, B.A. Matveev, M.A. Remennyi, A.A. Usikova. Infr. Phys. Technol., **117**, 103867 (2021). DOI: 10.1016/j.infrared.2021.103867

[16] N.D. Il'inskaya, A.A. Pivovarova, Ye.V. Kunitsyna, YU.P. Yakovlev. *Sposob izgotovleniya fotoelektricheskikh preobrazovateley na osnove mnogosloynoy struktury.* Pat. № 2783353, Rossiyskaya Federatsiya, prioritet izobreteniya 10 marta 2022 g. (in Russian).

[17] https://www.hamamatsu.com/content/dam/hamamatsu-photonics/sites/documents/99_SALES_LIBRARY/ssd/si_pd_kspd 9001e.pdf, p. 4.

[18] C.E. Housecroft, E.C. Constable. *Chemistry: An Integrated Approach* (Addison Wesley Longman Ltd., London, 1997).

[19] *Metallurgiya blagorodnykh metallov,* pod red. L.V. Chugaeva (M., Metallurgiya, 1987) p. 80. (in Russian).

[20] https://www.hamamatsu.com/content/dam/hamamatsu-photonics/sites/documents/99_SALES_LIBRARY/ssd/p10090-01_etc_kird1099e.pdf, p. 3.

Translated by E. Potapova